







Landslide on glaciers: an example from Western Alps (Cogne - Italy)

FRASCA Marco¹  <https://orcid.org/0000-0002-6466-600X>; e-mail: marcofrasca@hotmail.it

VACHA Damiano^{2*}  <https://orcid.org/0000-0001-9290-5912>;  e-mail: damiano.vacha@unito.it

CHICCO Jessica²  <https://orcid.org/0000-0001-6877-5425>; e-mail: jessica.chicco@unito.it

TROILO Fabrizio¹  <https://orcid.org/0000-0002-6386-3335>; e-mail: ftroilo@fondms.org

BERTOLO Davide³  <https://orcid.org/0000-0001-6860-2962>; e-mail: d.bertolo@regione.vda.it

*Corresponding author

1 Fondazione Montagna Sicura, Località Villard de la Palud 1, 11013 Courmayeur, Aosta, Italy

2 Università degli Studi di Torino, Department of Earth Sciences, Via Valperga Caluso 35, 10125 Torino, Italy

3 Regione Autonoma Valle d'Aosta - Assessorato alle opere pubbliche, territorio ed edilizia residenziale pubblica, Località Amérique, n. 33, 11020 Quart, Aosta, Italy

Citation: Frasca M, Vacha D, Chicco J, et al. (2020) Landslide on glaciers: an example from Western Alps (Cogne - Italy). *Journal of Mountain Science* 17(5). <https://doi.org/10.1007/s11629-019-5629-y>

© Science Press, Institute of Mountain Hazards and Environment, CAS and Springer-Verlag GmbH Germany, part of Springer Nature 2020

Abstract: In the warm summer of 2017, a landslide failed from the south-east side of the Col des Clochettes on the top of the underlying Trajo Glacier. The study area is at an elevation of about 3500 m a.s.l. in the Gran Paradiso Massif and can be hardly reached by walking from Cogne (Aosta Valley, NW Italy). Studies conducted by field surveys, photogrammetry (structure from motion) and satellite images analysis, integrated with the evaluation of data from meteorological stations have been used to reconstruct the phenomenon and infer its causes. The site is very complex to be studied especially due to logistic problems, therefore, measurements and observations that are common practice in other landslides are very difficult to apply here. So, many of the results achieved are not adequately supported by field studies. Anyway, the following factors could have affected the stability of the slope: i) the tectonic structure of the area, which is reflected on the morphology and on the geomechanics

characteristics of the rock masses; ii) the meteorological conditions during 3 months before the main failure, resulting in an extremely high temperature compared to historical data. Moreover, the analysis of multitemporal satellite images allowed to recognize that it was not a single landslide but that the phenomenon is articulated over time in at least five failures in about 2 months. Moreover, several predisposing factors may have been playing an important role in causing the instability: the degradation of permafrost (probably affecting rock mass due to the circulation of warm air and water in the discontinuity systems), the alternance of the freeze-thaw cycles and the availability of a considerable amount of water from rainfalls and nival fusion infiltrating deeply in the rock mass. More common causes such as rains and earthquakes have been excluded.

Keywords: Landslide; Glacier; Remote sensing; Climate changes; Western Italian Alps

Received: 13-Jun-2019

1st Revision: 17-Jul-2019

2nd Revision: 19-Dec-2019

Accepted: 01-Mar-2020

Introduction

The climate change can have great effects on slope stability, especially at elevations greater than 3000 m a.s.l., due to permafrost degradation, enhanced periglacial activity, increased precipitations, snowmelt and groundwater fluctuation (Crozier 2010; Gariano and Guzzetti 2016; Coe et al. 2018). As a demonstration, the literature reports an increase in the frequency of these events (Fischer et al. 2012). Therefore, the analysis of a case study in such remote locations is absolutely crucial for describing the evolution of high mountain slopes and for understanding how these fragile territories could couple with those changing conditions.

For these reasons, a landslide (Figure 1), observed during the annual summer campaign of the Italian Glaciological Committee (C.G.I.) on the Trajo Glacier in the Mount Grivola area, is described. Several hours of walk on a rambling path, a part of which on the glacier, are required to reach the landslide from the village of Epinel (1452 m a.s.l.). The landslide occurred, between spring and summer, in the median sector of the south-east (SE) slope of the Col des Clochettes rocky ridge, near the bivouac Balzola (3477 m a.s.l.). Coordinates of the centroid of the landslide are 45°36'15.90"N 7°16'39.34"E).

Direct observations, photogrammetrical reconstruction, multitemporal satellite image analysis and meteorological data analysis were used for the landslide characterization. As a result, the morphometry and the structural setting of the landslide area and its surroundings are investigated, the sedimentological characteristics of the deposit are resumed and the process evolution is described.

This study highlights the tectonic structure control on the morphology and the geomechanical features of the rock mass and reveals the main predisposing factor for the landslide instability together with the anomalous climatic trend before the event, suggesting it as the most probable triggering cause.

1 Geological and Geomorphological Framework

The landslide occurred on the M. Grivola, located on the northern side of the Gran Paradiso Massif (4061 m a.s.l., Graian Alps), along the divide between Valsavarenche and Cogne valleys. The slope is located on the SE side of a narrow and elongated rocky ridge, at about 3500 m a.s.l. On the SE side of the saddle, the slope shows a concavity reflecting past gravitative phenomena.

The Trajo Glacier is a “valley” or “alpine type” glacier characterized by a single tongue that occupies the large sub-elliptical collector basin (with SW-NE orientation) bordered by the high, steep and jagged rock ridges. The glacial mass develops in a SW/NE direction for about 2.9 km and reaches a maximum width of 1.16 km (in 2017). Glacier measurements, suspended since 1997, were resumed in 2009 and highlight the retreat (more than 250 m from 1999) of the glacier above the rocky leap (2890 m a.s.l.) occupied in the past by a massive serac. Thickness can be estimated greater than 50 m by direct observation into some crevasses. The left of the glacier is covered by an almost continuous debris layer due to the degradation of the ridge.

In the study area the bedrock is represented (Figure 2, from ISPRA 2015) by ophiolitic units

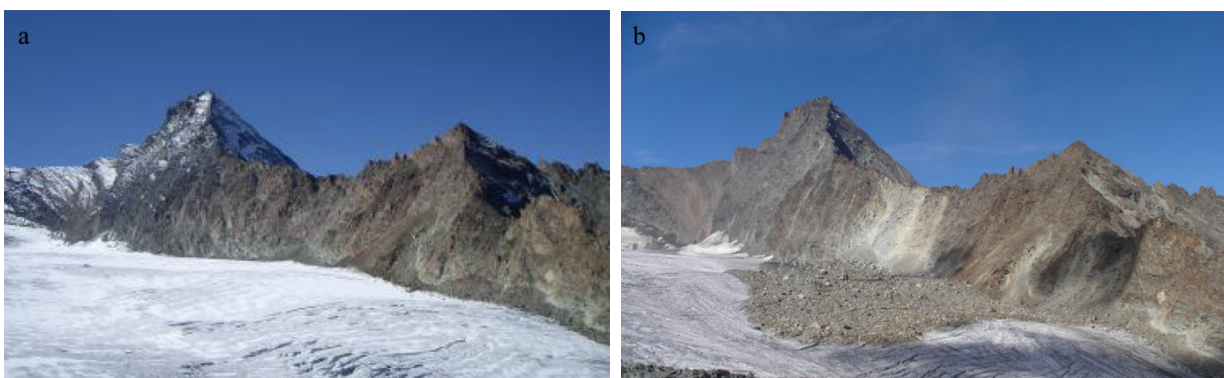


Figure 1 South-east (SE) slope of Col des Clochettes ridge before the rockfall (a) and after the event (b) (www.gulliver.it).

with alpine metamorphism in eclogitic facies (Green Schists), called Grivola-Urtier Unit (GRV), consisting of eclogitic metabasites, prasinites, chloritic schists and metagabbri (GRV_b). The Grivola-Urtier unit is in contact with the Grand Nomenon (GNM) and Rovenaud (RVN) units through the high-angle faults of the Belleface-Traio System, surrounded by the Traio marbles (TRJ) and Belleface Calcschists units (BLF). In detail, the rocks in which the landslide is developed are prasinites, characterized by a layering dipping about 55° towards N-NW and are faulted by lineaments oriented transversely to the saddle and characterized by a high dip value and NW-SE direction.

2 Methodology and Landslide Description

The study couples field observations, satellite images and orthorectified aerial photographs analysis through geomatics tools (Giuliani et al.

2016; Filipello et al. 2010; Mandrone et al. 2009). A digital model of the landslide zone was produced (from photos acquired from a helicopter) using techniques of structure from motion. It was realized to better reproduce the morphology, morphometry, sedimentological features and the structural framework of the area surrounding of the landslide (Figure 3). The photogrammetric survey was realized using 144 overlapping images acquired with a Canon PowerShot G15 (resolution 4000×3000 pix; 6 mm focal length; 1.86×1.86 pixel size) at a mean flying altitude of 500 m. Thirteen ground control points for the external orientation of the model, materialized by painting on visible rock faces, were placed at the perimeter of the landslide body and were measured using a rugged GPS tablet (Leica CS25 plus) able to reach a positioning error below 2 cm in the real-time RTK mode. *Photoscan*® software was used to perform tie point extraction, bundle-block adjustment, dense image matching, and 3D reconstruction. A 20 cm resolution DEM was therefore produced.

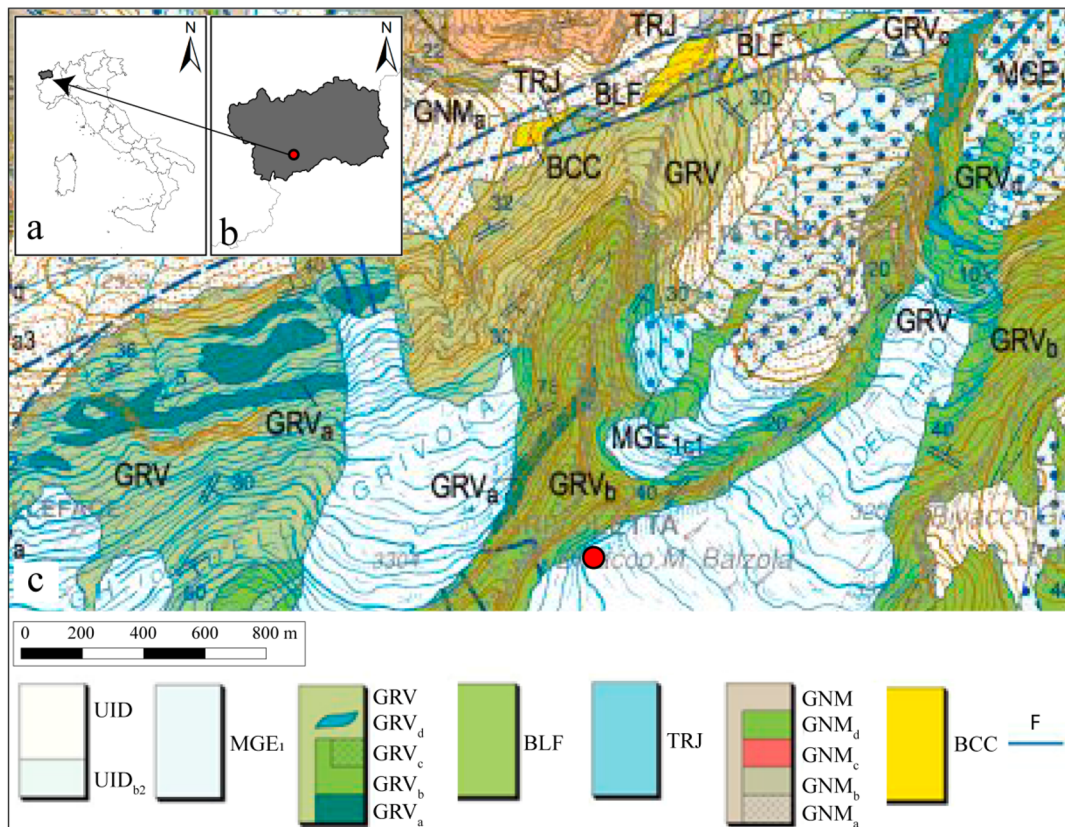


Figure 2 (a) position of the Aosta Valley Region; (b) location of the landslide in the Aosta Valley Region; (c) Geological map, from Geological map of Italy “Foglio 090 – Aosta” (scale 1:50.000) (ISPRA 2015). Legend: UID: recent deposits; UID_{b2}: colluvium; MGE₁: till and moraine deposits; GRV: Grivola-Urtier unit; BLF: Belleface Calcschists; TRJ: Traio Marbles; GNM: Grand Nomenon Complex; BCC: carbonatic breccias (Carniole Auct); F: Fault. The centroid of the landslide is highlighted with a red circle, 45°36'15.90"N, 7°16'39.34"E (UTM zone 32N).

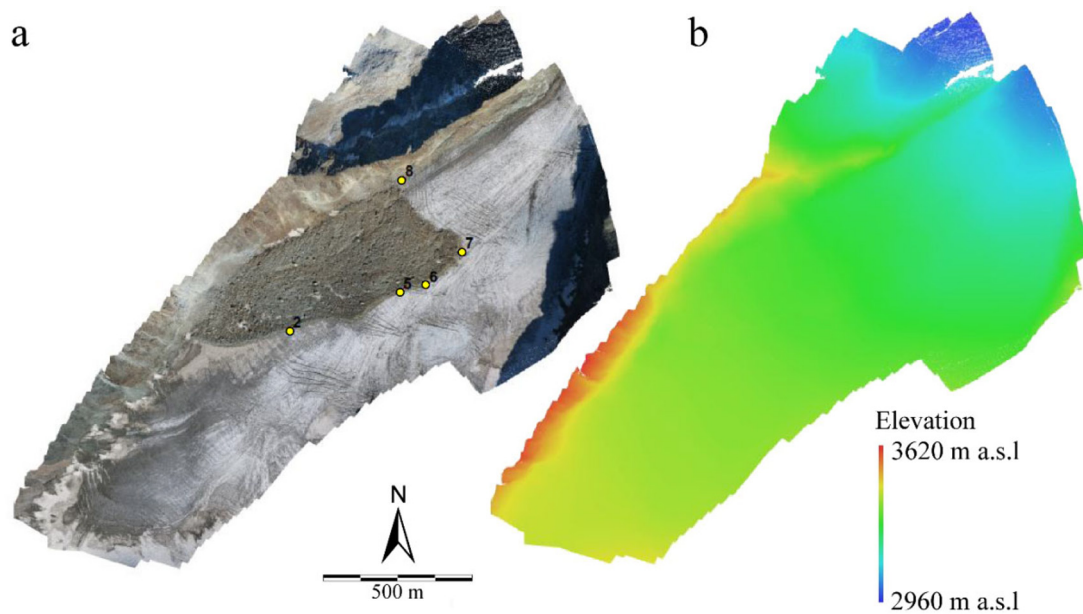


Figure 3 (a) Orthophoto and (b) Digital Elevation Model of the landslide. Numbered dots represent the five ground control points used for the model external orientation.

Moreover, a high-resolution orthophoto with a Ground Sample Distance (GSD) of 13 cm/pixel was generated. The final model has a mean reprojection error on check-points equal to 1 m, fully acceptable for the desired purposes.

The landslide interested a very steep rocky slope with a SE exposure. The top of the study area is on the ridge at an elevation of about 3500 m a.s.l. and the main scarp reaches the bottom of the slope at 3300 m where is located the glacier surface (Figure 4 and 5). The depletion zone covers an area of approx. 0.04 km² and its width along the ridge line is about 200 m. The crown is asymmetric and this is directly related to the arrangement of the tectonic lineaments and discontinuities. The accumulation zone follows the valley direction travelling on the very flat surface of the glacier (about 8°) for about 900 m where the front stops at about 3200 m of elevation. Figure 4 is realized by integrating field mapping and satellite images analyses. In particular, after drawing the perimeter of the landslide at every temporal stage, this feature was verified on the field as a double-check.

2.1 Evolution in time

To reconstruct the dynamic evolution of the landslide over time, multispectral satellite images of the ESA (European Space Agency) Sentinel-2

mission were analyzed. These images are characterized by a maximum resolution equal to 10, 20 and 60 m depending on the band, and snap the same point on the Earth's surface with the same viewing angle every 5 days. It was the only way to reconstruct the temporal evolution of the slope because it was not possible to observe the site from accessible places.

The landslide has developed over time in at least five enlarging events that have affected a continuously increasing area (already depicted in Figure 3) and therefore is the result of different small events that occurred in the period between 10/05/2017 and 14/07/2017. In Figure 6 are shown the details referred to the study areas in 6 step time, before and after the 5 events of 2017:

1. Pre-landslide conditions;
2. The first sign of the incipient failure of the slope can be dated between 10/05/2017 and 30/05/2017, highlighted by a niche on the slope and by a small new debris deposit on the glacier surface (white);
3. Subsequently, between 31/05/2017 and 09/06/2017, the debris deposit at the bottom of the slope increase in a barely noticeable way on the satellite image, and can be appreciated looking at the weak contrast on the white color of the snow;
4. In the days between 10/06/2017 and 19/06/2017, there is a clear increase in the size of

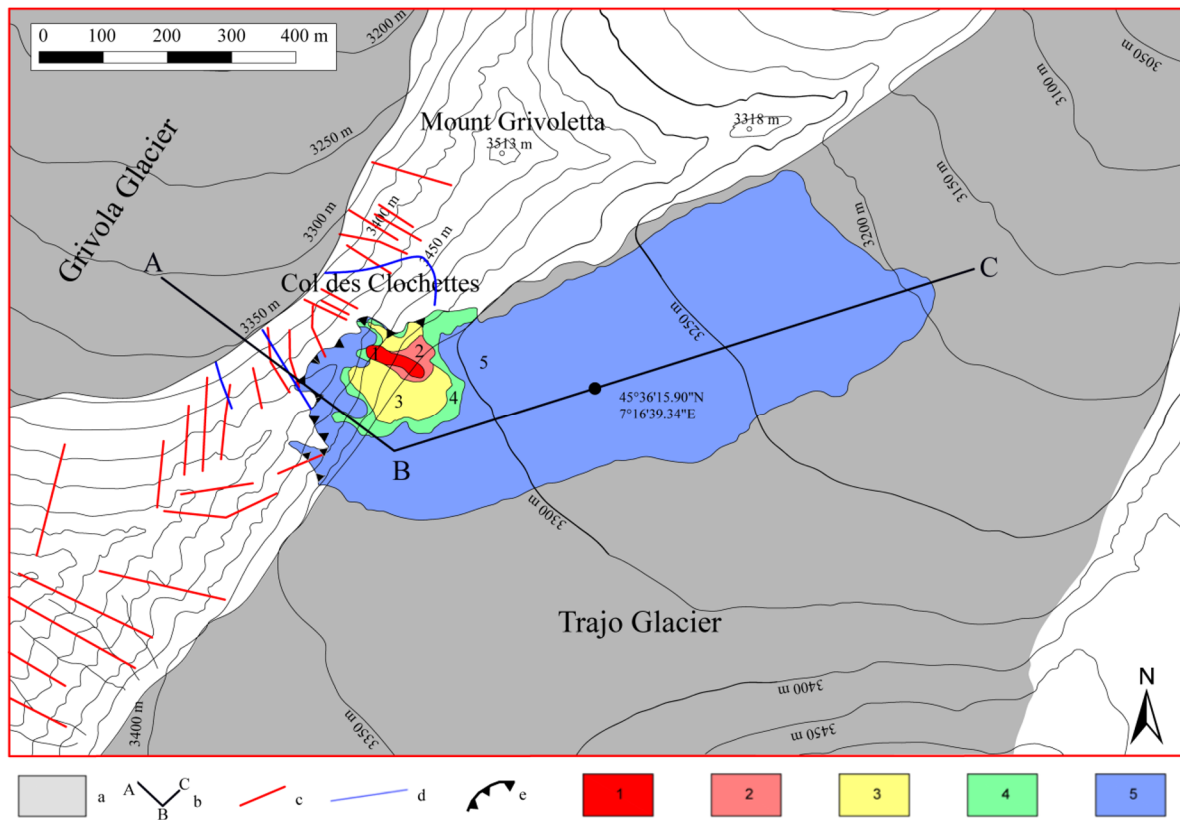


Figure 4 Detailed map of Col des Clochettes landslide evolution (3550 m a.s.l.). a) permanent snow and ice; b) cross-section profile A-B-C (see Figure 4); c) tectonic lineation; d) faults; e) main scarp. Different colors (1 to 5) highlight the temporal evolution of the rockfalls and the area interested by each event, from the first (10/05/2017) to the fifth (14/07/2017).

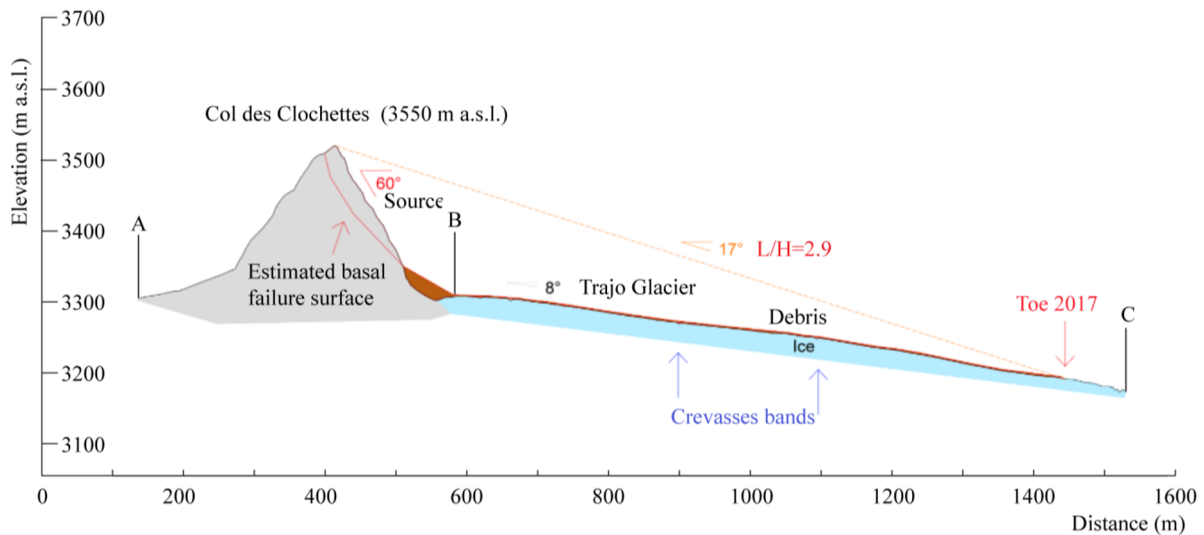


Figure 5 Sketch cross-section of Col des Clochettes landslide representing the situation at the end of its evolution in 2017 (for location see Figure 4). A, B and C are the vertex of the cross section-profile (Figure 4).

the detachment niche and the debris deposit;

5. Between 20/06/2017 and 04/07/2017, the niche interests a growing area of the slope and the

deposit at the bottom considerably increases, too;

6. The last and bigger collapse can be referred to the period between 05/07/2017 and 14/07/2017.

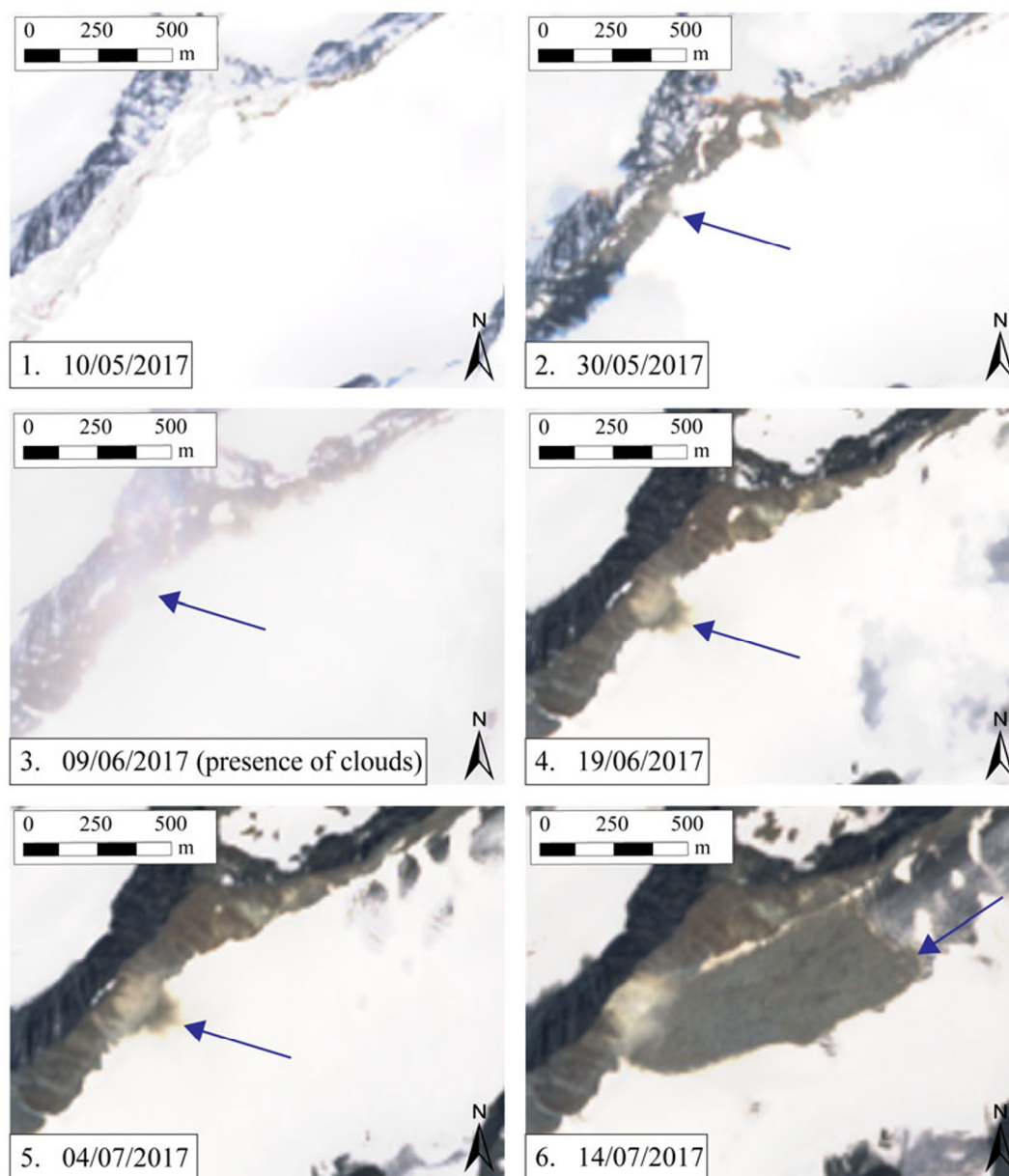


Figure 6 Dynamic evolution of the landslide over time by satellite images of the ESA (European Space Agency) Sentinel-2 missions. Arrows highlight the tip of the landslide at every time step.

2.2 The source area

The rock mass consist of prasinite, a basic metamorphic rock in greenschist facies with minute grain and variable texture, characterized by a massive structure with a schistosity (about 1 m spacing, from field observation) dipping steeply toward N-NW, estimated 55/323 (SC) intersecting with a high angle the SE front of the ridge that it is oriented 60/120 (F). On the divide, in correspondence of the crown, the orthophoto and the 3D model referred to the pre-landslide

situation shows the presence of an elongated trench (length 120 m) along the top of the ridge. The trench was highlighted on the ground by the persistence of snow cover in periods when other sectors of the slope was already completely clear. This morphological element is an unequivocal sign that precursors movements occurred for a long time. Moreover, this depression probably acted as a preferential way of water infiltration in rock masses.

The rock mass is segmented, in addition, by a set of discontinuity (K1) characterized by an

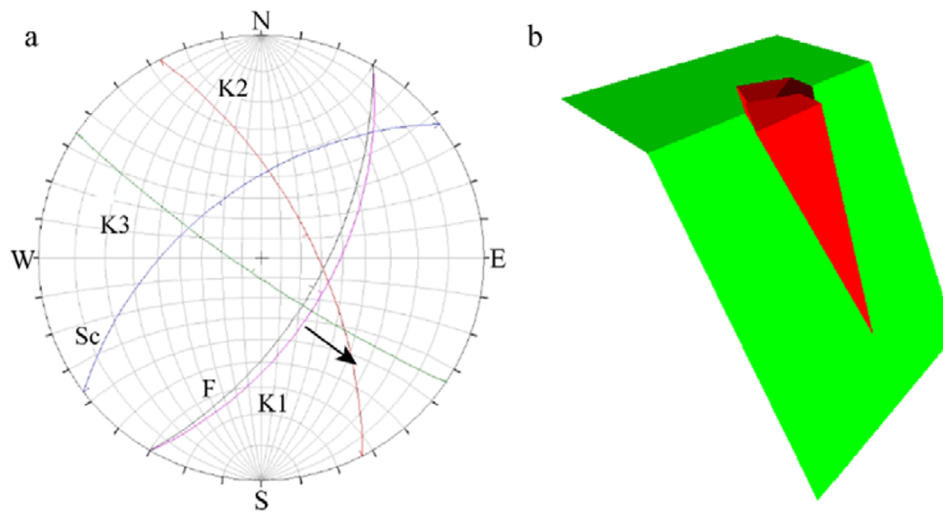


Figure 7 Stereonet of the main discontinuity systems identified by photointerpretation (a) and perspective view of the kinematics (b). Keys: front (F), schistosity (Sc), secondary fracturation (K1), other discontinuity systems (K2, K3). The arrow highlights the direction of potential failure of the wedge formed by K2 and K3 jointing systems. For (b): green colour represents the ridge (face and top), red colour highlights the unstable wedge.

average spacing of 10 m (estimated from aerial images), almost orthogonal to the schistosity, oriented about 55/120; this system determines the slope inclination. Thus, the rock mass consists of a series of portions and fragments of sounding rock, separated by open joints with filling materials that are the product of the alteration and degradation of joints surfaces. Observation on fallen blocks highlights that joints surfaces are rather smooth with iron-stained surfaces with many pieces of evidence of extensive water circulation.

At a larger scale, the ridge is crossed by a series of faults and discontinuities characterized by a much greater length than the systems identified previously (hundred meters). Using orthorectified aerial photographs and DTM models, it was possible to clearly identify the presence of at least two main systems forming a wedge able to failure (K2 - 64/63 and K3 - 81/214). It is possible to clearly identify (Figure 7, output from *Dips*® by Rocscience) the wedge, formed by K2 and K3 which slides along a SE direction (Hoek and Bray 1981; Filipello et al. 2015). The shape of the wedge represents perfectly that of the landslide.

2.3 The deposit

The areal extension of the deposit, based on observations on the Sentinel-2 satellite image of 07/09/2017, is estimated in 0.236 km² (Bessette et al. 2018): its maximum length is 870 m and the

maximum width is 320 m at the front. The deposit shows an elongated lobe that turns abruptly on the left touching the glacier and develops longitudinally along the line of maximum slope. It has unusual L/D ratio, with an elongation much greater than elevation due to the high mobility on the material over the glacier. During the transport, the debris has generated a continuous accumulation of firn on the glacier perimeter scraped from the surface of the ice.

The surface of the deposit has characteristics typical of rockfall on glaciers that are not common in other types of landslides. Longitudinal strips/furrows (Deline 2001), clearly visible in the central and lower sectors of the deposit, have been interpreted in the literature as cutting zones between adjacent areas that move independently and also as a break in granular flow when the landslide spreads. In both cases, the furrows probably indicate the dominant role of inertia (Dufresne & Davies 2009) with respect to lateral resistances. Since they are probably "fossilized" cutting or breaking regions or both, they need a "soft" and low-friction base to be stored after a long travel distance (De Blasio 2014).

The average thickness of the accumulation, measured directly in the field, is relatively small (about 1.5 m), this is in agreement with similar observation (Shugar & Clague 2011). It consists of an extremely heterogeneous deposit, from boulders a few meters wide (the largest block has a volume

of about 2000 m³) to centimetric pebbles, made by angular rock fragments. The deposit can be divided into three sectors, roughly bordered by two bands of open crevasses present on the surface of the glacier, characterized by rock debris with decreasing dimensions towards the distal sector (Figure 8):

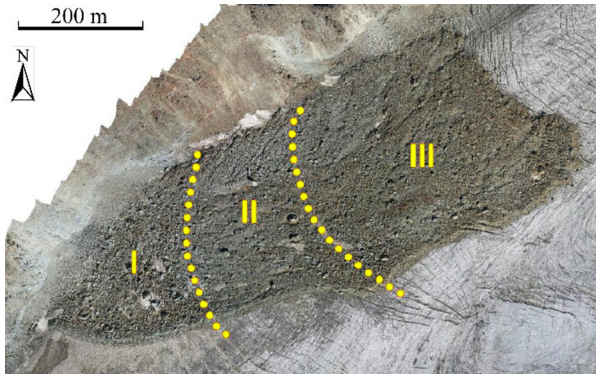


Figure 8 Orthoimage of the debris deposit on glacier surface (September 2018): the scarp of the landslide is on the left of the image. The three sectors with different kind of deposits are highlighted in yellow.

- “Sector I”, the deposit has a larger size than the other two sectors, and it is characterized by the presence of many blocks of decametric dimensions (more than 4 big blocks each 10.000 m²);
- “Sector II” is characterized by a general uniformity in size of the deposit but, some isolated large blocks are still present (2 big blocks each 10.000 m²): it is characterized by a slight local increase in the slope of the glacier surface evidenced by the presence upstream and downstream by two bands of open crevasses.
- “Sector III” has characteristics that are substantially similar to Sector II, where, however, just a few large blocks appear (less than 1 block each 10.000 m²).

On the left side of the deposit front, it is possible to observe a small slide that occurred some time after the debris mass has stopped.

2.4 Evolution of the deposit on the glacier

It is possible to observe phenomena affecting the deposit and causing its evolution after the main deposition, by comparing images immediately after the collapse (19/07/2017) and others about 100 days later (01/11/2017) (<https://apps.sentinel-hub.com/sentinel-playground>). These include: i) the complete fusion of the “scraped” firn

accumulation from the surface of the glacier and deposited on the perimeter of the debris deposit, ii) a principle of the phenomenon of differential ablation that began to affect the glacial mass, iii) a kind of “fluidification” of the deposit, iv) the detachment of a small portion of debris from the front, v) the sliding of boulders and blocks on the glacier.

Differential ablation, due to a different melting speed of the ice covered by the debris with respect to the surrounding areas, causes the deposition area to be topographically “raised” compared to the surrounding zones to which it is connected with a morphological “step” (Reznichenko et al. 2011). Moreover, can be noticed that the deposit - in its middle-lower sector - has undergone a “fluidification”, highlighted by the presence of furrows and stripes, not present in the middle-upper part. This aspect could probably be due to following rainy events and to the merger of the superficial firn.

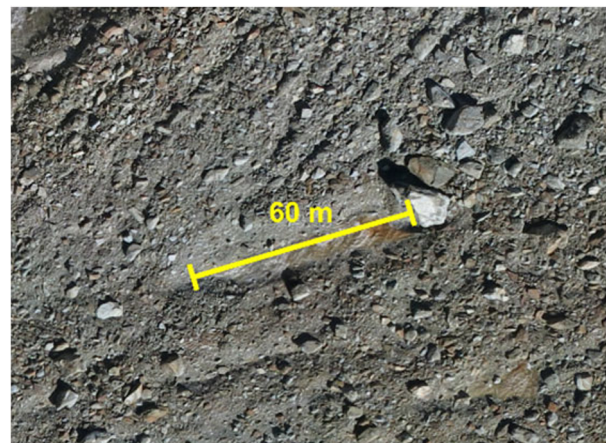


Figure 9 Detail of the sliding strips of a boulder on the surface of the glacier.

Also, the movement of some blocks and boulders, highlighted by the presence of large and long furrows and stripes on the surface of the glacier, is probably related to rainfalls that affected metastable blocks. Two of these strips are clearly visible in the aerial images of the deposit (Figure 9): they are connected to blocks that expose the basal layer of ice below. The largest one (about 10 m×16 m) has a strip length of 60 m. The absence of impact signs on the deposit excludes the hypothesis that the blocks may have fallen after the main collapse, impacting and rolling on the deposit and then transforming its motion into a slip.

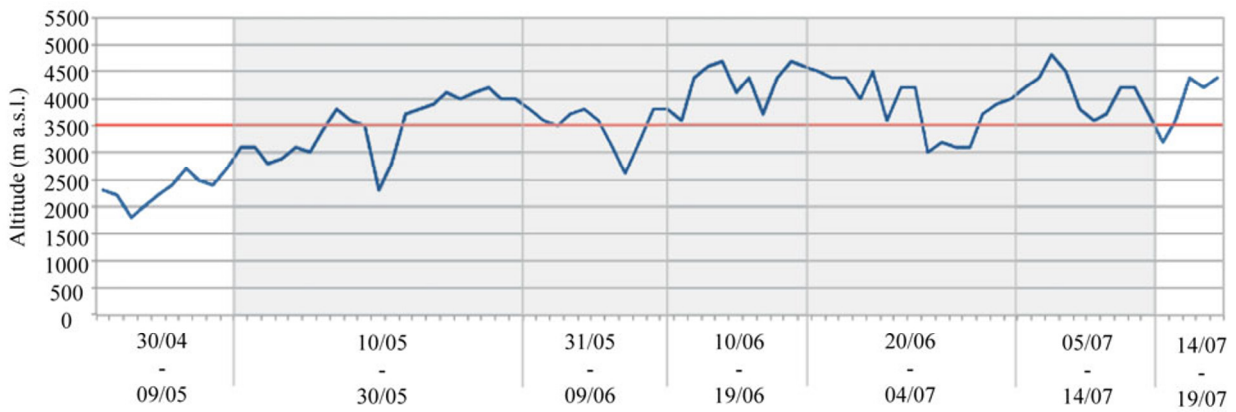


Figure 10 Reconstruction of the altitude of the thermal zero in the free atmosphere at the 5 activation of the landslide. Red line is the elevation of the crown. (Dates are referred to 2017)

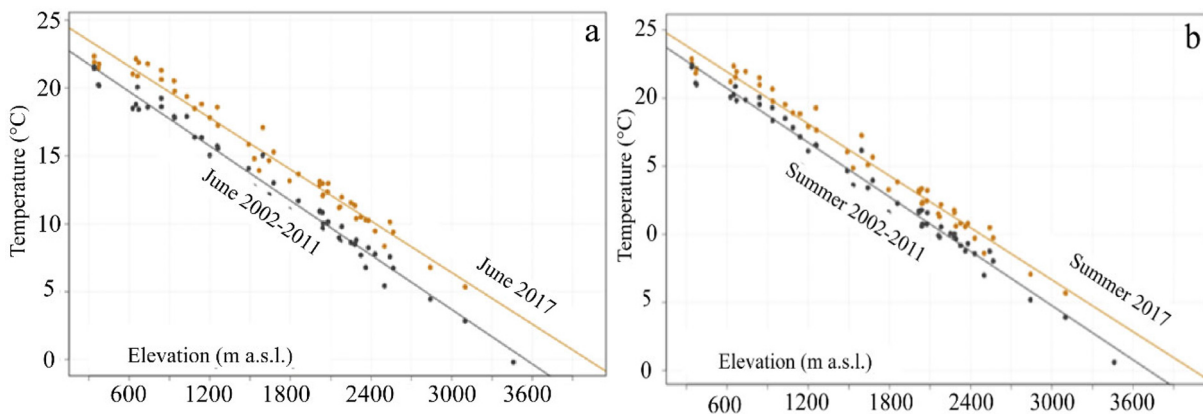


Figure 11 (a) Comparison between temperature in June 2017 (yellow) with the average temperature in June in the period 2002-2011 (blue) at different elevations (<http://cf.regione.vda.it/temperature.php>). (b) Temperature comparison referred to summer season.

3 Discussion

Investigating the causes of a high-altitude instability phenomenon linked to climatic variations is rather complex both from a logistical and technical point of view (Huggel et al. 2012; Kuhle 2007).

For example, air temperature at the crown should be known as well as temperature in depth in the rock mass, but these parameters are quite difficult to determine and measures are rare, discontinuous and scattered all over the world (Vagnon et al. 2019; Chicco et al. 2019). Therefore, in order to hypothesize the local climatic setting, the trend of air temperature at the altitude of the landslide (3500 m a.s.l.) must be estimated. In Figure 10 the altitude of the daily thermal zero calculated for the months of April, May, June and July 2017 is shown (from the Daily meteorological

Bulletins by the Regional Functional Center). This is an experimental datum obtained from a physical-mathematical model that covers the whole region representing the average daily value. The thermal zero stands at an elevation of 3000 m or lower until the 15th of May, then it rises above 3500 m for almost nine weeks, in which the five rockfalls occurred. Moreover, Figure 11, showing thermal data against elevation (referred to data collected by Regione Valle d’Aosta: <http://cf.regione.vda.it/home.php>.) depicts how June 2017 was sensibly warmer than the average in the period 2002-2011. Also looking at the whole summer 2017, thermal data versus elevation are exceptionally high respect to the period 2002-2011.

As a matter of fact, according to Davies et al. (2001) and Fischer et al. (2013), there are no other causes except that anomalous high temperature to be invoked as the triggering factor for this landslide. In fact, correlating cumulated daily

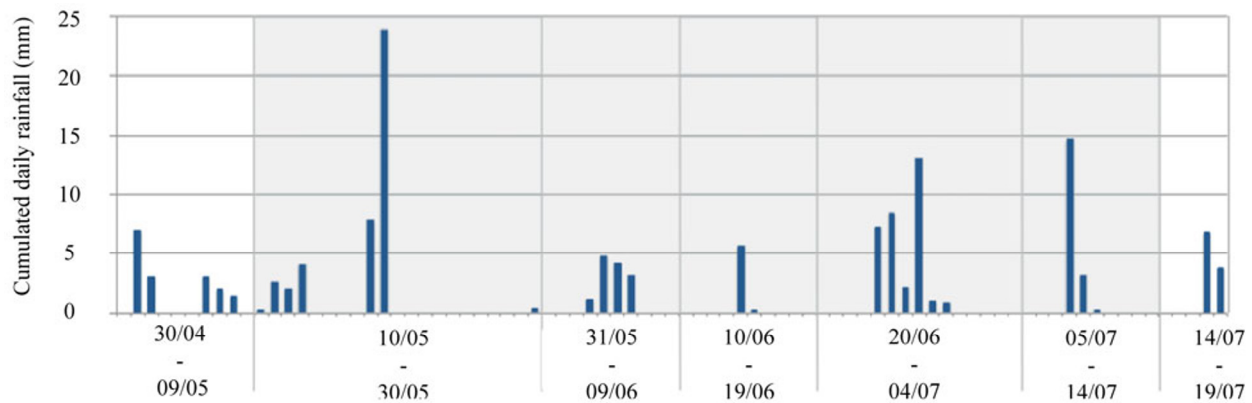


Figure 12 Cumulated daily rainfall for the Cogne-Valnontey weather station at the 5 activation of the landslide (Grey colours indicate the period of activation of the landslide.) (Dates are referred to 2017.).

rainfall from the Cogne-Valnontey weather station (less than 6 km from the landslide but at about 2000 m a.s.l.) with the five rockfall events (Figure 12) it is possible to observe how each of the reactivation correspond to cumulated daily rains lower than 25 mm. These quantities are absolutely normal. Also, earthquakes are not reported in the area, so the two most common triggering factors seems not to be responsible for this landslide. Of course, it is difficult to demonstrate this statement without field data, but all clues go in this direction. More and more these events are recorded in Italian alps and probably in a few years a database will be available and statistics could help scientist in depicting this climatic change.

4 Conclusions

In summer 2017, a landslide interested the steep slope above the right side of the Trajo Glacier. The deposit, running above snow and ice, is characterized by high mobility, travelling on a flat slope (about 8°) for nearly 1 km. According to Varnes (1978), it can be classified as multiple rockfalls evolving (in space and time) into a rock avalanche for about half million m³ as total displaced material (Mandrone 1995).

The study highlighted that many elements

contributed to the instability:

- The main predisposing factor is the tectonic structure, which is reflected on the morphology and on the geomechanics characteristics of the rock masses, characterized by many discontinuity sets forming potentially unstable wedges;
- The most probable triggering factor can be identified with the climatic trend before the event, characterized by an anomalous temperature, in particular in June that is in line with the maximum temperatures recorded in the past.

The failure was probably triggered by the interaction of several factors all connected to anomalous high temperature: I) the degradation of permafrost, II) the alternance of the freeze-thaw cycles, III) the availability of a considerable amount of meteoric water and water from nival fusion and IV) high rate of infiltration due to the jointing of the rock mass.

Acknowledgments

Thanks to Marta Chiarle and Giovanni Mortara for the precious information; Piero Borre and Chiara Caminada for sharing a beautiful experience in a unique mountain context and for the patient help offered; Prof Giuseppe Mandrone for the correction of the manuscript and for the encouragement to publish.

References

Bessette-Kirton EK, Coe JA, Zhou W (2018) Using stereo satellite imagery to account for ablation, entrainment, and compaction in volume calculations for rock avalanches on

glaciers: Application to the 2016 Lamplugh rock avalanche in Glacier Bay National Park, Alaska. *Journal of Geophysical Research: Earth Surface* 123: 622-641.

- <https://doi.org/10.1002/2017JF004512>
- Chicco JM, Vacha D, Mandrone G (2019) Thermo-physical and geo-mechanical characterization of faulted carbonate rock masses (Valdieri, Italy). *Remote Sensing* 11(2): 179. <https://doi.org/10.3390/rs11020179>
- Coe JE, Bessette-Kirton EK, Geertsema M (2018). Increasing rock-avalanche size and mobility in Glacier Bay National Park and Preserve, Alaska detected from 1984 to 2016 Landsat imagery. *Landslides* 15: 393-407. <https://doi.org/10.1007/s10346-017-0879-7>
- Crozier MJ (2010) Deciphering the effect of climate change on landslide activity: a review. *Geomorphology* 124:260–267. <https://doi.org/10.1016/j.geomorph.2010.04.009>
- Gariano SL, Guzzetti F (2016) Landslides in a changing climate. *Earth-Science Reviews* 162:227–252. <https://doi.org/10.1016/j.earscirev.2016.08.011>
- Davies MCR, Hamza O & Harris C (2001) The effect of rise in mean annual temperature on the stability of rock slopes containing ice-filled discontinuities. *Permafrost Periglacial Processes* 12: 137-144. <https://doi.org/10.1002/ppp.378>
- De Blasio FV (2014) Friction and dynamics of rock avalanches travelling on glaciers. *Geomorphology* 213: 88-98. <https://doi.org/10.1016/j.geomorph.2014.01.001>
- Deline F (2001) Recent Brenva rock avalanches (Valley of Aosta): new chapter in an old story? *Supplementi Geografia Fisica & Dinamica Quaternaria V*: 55-63.
- Dufresne A, Davies TR (2009) Longitudinal ridges in mass movement deposits. *Geomorphology* 105 (3-4): 171-181. <https://doi.org/10.1016/j.geomorph.2008.09.009>
- Filipello A, Giuliani A, Mandrone G (2010) Rock slopes failure susceptibility analysis: from remote sensing measurements to geographic information system raster modules. *American Journal of Environmental Sciences* 6(6): 489-494. <https://doi.org/10.3844/ajessp.2010.489.494>
- Filipello A, Mandrone G, Bornaz L (2015) Structural data treatment to define rockfall susceptibility using long range laser scanner. In: G. Lollino et al. (eds.), *Engineering Geology for Society and Territory – Volume 6*. pp 721-724. https://doi.org/10.1007/978-3-319-09060-3_129
- Fischer L, Purves RS, Huggel C, et al. (2012) On the influence of topographic, geological and cryospheric factors on rock avalanches and rockfalls in high-mountain areas. *Natural Hazards and Earth System Sciences* 12: 241-254. <https://doi.org/10.5194/nhess-12-241-2012>
- Fischer L, Huggel C, Kääh A, Haeberli W (2013) Slope failures and erosion rates on a glacierized high mountain face under climatic changes. *Earth Surface Processes and Landforms* 38: 836-846. <https://doi.org/10.1002/esp.3355>
- Giuliani A, Filipello A, Mandrone G (2016) Extreme gis applications for 3d visualization aimed to geological and mining modelling. *Italian Journal of Engineering Geology and Environment* 2: 31-39. <https://doi.org/10.4408/IJEGE.2016-01.O-03>
- Hoek, E, Bray JW (1981) *Rock Slope Engineering*. 3rd Ed., Spon Press, London. p 368.
- Huggel C, Zraggen-Oswald S, Haeberli W, et al. (2005) The 2002 rock/ice avalanche at Kolka/Karmadon, Russian Caucasus: assessment of extraordinary avalanche formation and mobility, and application of QuickBird satellite imagery. *Natural Hazards and Earth System Science*. 5(2): 173-187. <https://doi.org/10.5194/nhess-5-173-2005>
- Huggel C, Allen S, Deline P, et al. (2012) Ice thawing, mountains falling are alpine rock slope failures increasing? *The Geologists' Association & The Geological Society of London, Geology Today*, Vol. 28, No. 3, May–June. pp 98-104. <https://doi.org/10.1111/j.1365-2451.2012.00836.x>
- Kuhle M (2007) Altitudinal levels and altitudinal limits in high mountains. *Journal of Mountain Science* 4(1):24-33. <https://doi.org/10.1007/s11629-007-0024-5>
- ISPRA (2015) - Carta Geologica d'Italia alla scala 1:50.000: Aosta Foglio 090 (In Italian).
- Mandrone G (1995) - Valutazione del rischio di frana nella media Valtournenche (Fieraz-Valle d'Aosta). *GEAM dicembre 1995*. (In Italian).
- Mandrone G, Buratti L, Chelli A, et al. (2009) A large, slow moving earth flow in the northern Apennines: the Signatico landslide (Italy). *Geografia Fisica & Dinamica Quaternaria* 32 247-253.
- Reznichenko NV, Davies TRH, Alexander DJ (2011) Effects of rock avalanches on glacier behavior and moraine formation. *Geomorphology* 132 (2011) 327–338. <https://doi.org/10.1016/j.geomorph.2011.05.019>
- Shugar H, Clague J (2011) The sedimentology and geomorphology of rock avalanche deposits on glaciers. *Sedimentology* 58(7): 1762-1783. <https://doi.org/10.1111/j.1365-3091.2011.01238.x>
- Vagnon F, Colombero C, Colombo F, et al. (2018) Effects of thermal treatment on physical and mechanical properties of hydrothermally metamorphosed Lausa limestone (NW Italy). *International Journal of Rock Mechanics and Mining Sciences* 116 (2019) 75-86. <https://doi.org/10.1016/j.ijrmms.2019.03.006>
- Varnes DJ (1978) Slope Movements Types and Processes. In: Schuster R.L. & Krizek R.J. (Eds.) *Landslides: Analysis and Control*. Transportation Research Board Special Report 176. National Academy of Sciences, Washington. pp 11-33.